Microscale CFD Simulations of a Wind Energy Test Site in the Swabian Alps with Mesoscale Based Inflow Data

Microscale CFD Simulations of a Wind Energy Test Site in the Swabian Alps with Mesoscale Based Inflow Data

Patrick Letzgus[1], Asmae El Bahlouli[2], Daniel Leukauf[3], Martin Hofsäß[4], Thorsten Lutz[1] and Ewald Krämer[1]

[1] University of Stuttgart, Institute of Aerodynamics and Gas Dynamics (IAG), Pfaffenwaldring 21, 70569 Stuttgart, Germany

[2] University of Applied Sciences Esslingen, Faculty of Building-Services-Energy-Environment

[3] Karlsruhe Institute of Technology (KIT), Institute of Meteorology and Climate Research, Atmospheric Environmental Research (IMK-IFU)

[4] University of Stuttgart, Stuttgart Wind Energy at Institute of Aircraft Design (SWE)

E-mail: patrick.letzgus@iag.uni-stuttgart.de

Abstract. The current study describes analyses of the WINSENT wind energy test site located in complex terrain in Southern Germany by highly resolved numerical simulations. The resolved atmospheric turbulence is simulated with Delayed Detached Eddy Simulations by the flow solver FLOWer without consideration of the research wind turbines.
The mean inflow and wind direction of the analysed time period is provided by precursor simulations of project partners. The simulation model chain consists of three codes with different time scales and resolutions. The model chain provides a data transfer from mesoscale WRF simulations to OpenFOAM. As a next step OpenFOAM provides inflow data in the valley of the terrain site for the present FLOWer simulations, the code with the highest resolution in space and time. The mean velocity field provided by OpenFOAM is superimposed with fluctuations that are based on measurements to obtain the small turbulent scales within the FLOWer simulations, which the previous tools of the model chain can not resolve.
Comparisons with the two already installed met masts clarify that the current FLOWer simulations provide an adequate agreement with measured data. The results are verified with the application of a second simulation, in which a homogeneous velocity profile is superimposed with turbulence. Thus, comparisons with measured data showed that the benefit of using the inflow data of this model chain is especially evident near the ground.

1. Introduction

The investigation of wind energy in complex terrain is an important part of the Southern German Research Cluster (WindForS) [1]. As part of the WindForS project WINSENT, a wind energy test site with two 750kW wind turbines and four meteorological (met) masts is currently under

construction in the Swabian Alps (Southern Germany) [2]. The wind energy test site shown in Figure 1 is characterised by a flat valley, a steep slope fully covered by a dense forest and a flat plateau on top of this slope, where the wind turbines will be installed. The steep slope of the complex terrain is intended to exploit the acceleration of the wind in order to generate more power [3, 4]. This leads to much more complex inflow conditions, which are characterised by larger inclination angles, changes of the wind shear profile and in general higher turbulence intensities [5, 6]. Significant numerical analyses of complex terrain sites have been conducted over the last few years via Computational Fluid Dynamics (CFD). The Bolund experiment serves as a validation for a large number of topographies of varying complexity [7]. The influence of forested hills was investigated and analysed by Finnigan and Belcher [8]. Applying Reynolds Averaged Navier-Stokes simulations, the general effects of topographies like an acceleration of the wind speed or the inclination of the flow field can be analysed [9]. Using hybridization of RANS and Large Eddy Simulations (LES), detached vortex structures and flow separation areas can be resolved while turbulence within attached boundary layers is still in RANS mode [10]. This point is a major advantage for microscale simulations of flows over complex topographies and is used for the current numerical study.

The present study deals with highly resolved microscale FLOWer simulations of a 10 minute time period on 09.12.2019. The research wind turbines are not part of this numerical study. The wind turbines will be considered in a next step. The results are compared to measurement data. This comparison shall validate the microscale simulations, as the next step requires a fully meshed wind turbine to be installed in the simulation domain to accurately analyse loads, power and near wake development of the wind turbines in the observed time period. The objective of the current study is to simulate and validate highly resolved turbulent inflow conditions for the wind turbines on the test site. The high resolutions in space and time of the FLOWer simulations are required for a correct prediction of the turbulent inflow of the wind turbines. Aeroelastic analyses of the wind turbine also require these fine spatial and temporal resolutions that are part of the WINSENT project, too. The inflow data is based on a three part simulation model chain starting from mesoscale simulations and ending with high fidelity FLOWer simulations. Previous CFD studies of the WINSENT test site with and without consideration of wind turbines have already been concluded in previous projects [2, 6, 11] and as part of the current project [12].

The WINSENT test field currently offers a wide range of measuring equipment such as ultrasonic anemometers and cup anemometers attached to the two already installed 100 metres (m) high met masts, lidar instruments and unmanned aerial system (UAS) measuring flights. Over an intense observation period (IOP), six lidar instruments, UAS measuring flights and fully equipped met masts simultaneously generated wind field data suitable for the validation of the simulations. The met masts are equipped with ultrasonic anemometers at 23m, 46m, 73m and 96m heights. Heated cup anemometers are placed at 10m, 45m, 59m, 72m, 86m and 100m heights. This paper is focused on the comparison of FLOWer simulations with met mast data in the observed time period based on inflow data provided by a mesoscale solver.

In section 2 the flow solver FLOWer, the model chain, the meshes and the general numerical setup are detailed. The numerical results will be shown and compared to measurements of the met masts. A summary of the main findings can be found in the conclusion.

2. Methodology

2.1. Model Chain and FLOWer Inflow

To consider atmospheric turbulence, FLOWer provides the possibility to either apply synthetic turbulence or to propagate transient inflow data from measurements or precursor flow simulations of other solvers.
For the current study a simulation chain consisting of three models is used. The initial data is provided by the mesoscale Weather Research and Forecasting Model (WRF) simulations from Karlsruhe Institute of Technology (KIT), Institute of Meteorology and Climate Research, Atmospheric Environmental Research (IMK-IFU) [13]. The WRF Model is driven by the model analysis of the European Centre for Medium-Range Weather Forecast (ECMWF). This data is provided at six hour intervals and is interpolated in time at the model boundaries. In this case, WRF, simulating the mesoscale wind flow over the test site on 09.12.2019, was used to drive an OpenFOAM URANS model with higher resolutions in space and time at University of Applied Sciences Esslingen, Faculty of Building-Services-Energy-Environment. The output of this model was in turn used as an inflow for FLOWer, the flow solver with the highest resolutions and order in space and time, which is used at the Institute of Aerodynamics and Gas Dynamics at the University of Stuttgart (IAG).
The model chain has two main objectives. Firstly, the local wind field analysis over longer time periods performed by the first two tools of the model chain. Thus, the wind turbine aerodynamics are not important and the microscale FLOWer simulations are not needed. Secondly, the fully numerical acquisition of the wind turbine aerodynamics under consideration of meteorological and topographic influences. Therefore, the wind field analyses of OpenFOAM are used to select interesting time periods for the wind turbines and simulate these conditions with FLOWer.
The spatial resolutions within the nested model chain increases continuously, whereas the domain size also becomes smaller due to the increasing computing costs. The horizontal resolution of the WRF model is 150m and the vertical resolution is 15m near the ground with a domain size of 45km $\times$ 45km. WRF is used in LES mode at this resolution, being aware that this grid spacing is quite coarse for LES. A three-dimensional turbulence kinetic energy (TKE) 1.5-order closure is used. The WRF model does not resolve the turbulence adequately, but this is not the goal of this stage of the model chain. The OpenFOAM domain extends over an area of 10km $\times$ 10km with a spatial resolution of maximum 20m and minimum 5m. The grid of the FLOWer simulations as shown in Figure 1 (a) depicts spatial resolutions of 1m in the areas of interest and the domain size is approximately 1.8km $\times$ 1.2km. The FLOWer grid is a fully structured mesh with hexagonal cells in every region.
OpenFOAM provides inflow data for the FLOWer simulations at the corresponding inflow plane that is visualised in Figure 1 (b). The simulation time period was selected between 2:40 pm and 2:50 pm because the OpenFOAM data showed only minor deviations in mean wind speed and wind direction compared to the met masts. Simulations of these short time periods are necessary to investigate loads and near wake of wind turbines with small time steps of approximately one azimuthal degree of the rotor blades. Larger periods of time can not be realized due to the immense computing costs. It is a day time period with neutral conditions. Hence, the boussinesq approximation was turned off and no buoyancy forces were applied. The wind conditions were quite typical for the shown test site, which means the wind speeds were slightly below rated conditions at the hub height (73m a.g.l) with relatively high turbulence intensities. The OpenFOAM inflow data was averaged due to very small fluctuations of the turbulence and negligible changes in wind speed and direction. This means the delivered inflow data does not change in time but varies spatially.
The resulting time averaged inflow plane is superimposed with synthetic turbulence extracted from measurement data of the met masts. The met mast data yielded a turbulence intensity of

16% at the hub height in the observed time period. Based on the measured turbulence intensity and previous parametric studies of the turbulence statistics, synthetic turbulence was generated and superimposed to the mean inflow in the valley. For the generation of the turbulence the Mann Model was used [14]. Through the application of this model it is possible to extract the fluctuations and turbulence cascades from specially measured turbulence situations in order to simulate the existing flow conditions. The model uses the length scale L the stretching factor Γ and the dissipation $\alpha\epsilon^{2/3}$ as input. The length scale of the synthetic turbulence was chosen based on findings of Peña [15] and is set to $L = 40$m at the hub height. The other parameters Γ and $\alpha\epsilon^{2/3}$ are set to 3.9 and 0.035. Subsequently, the turbulent fluctuations are modelled by performing an inverse Fourier Transformation using the Mann model Spectrum and the Gaussian random complex variable [6]. Thus, a time signal of turbulent fluctuations is created, which has then been superimposed with the time averaged flow data provided by OpenFOAM. The anisotropy of the superimposed turbulence is based on the IEC 61400-1 standard. The standard deviation of the lateral velocity is σ_v=0.7σ_u and of the vertical velocity σ_v=0.5σ_u. The resulting highly resolved unsteady turbulent inflow data with 1m resolution is transferred to FLOWer by a Dirichlet boundary condition. This inflow condition initializes all conservative variables (ρ,ρu,ρv,ρw,ρe) at the first cell of the mesh by transferring inflow values. The symbol ρ stands for density, u, v and w are the spatial velocity components and e constitutes the total energy. Thereby, the anisotropic turbulence typical for complex terrain sites can be propagated through the field. In the finest region of the domain the grid shows 40 cells per length scale, which is an adequate amount to resolve the turbulent structures with low dissipation while propagating the flow through the domain [16]. The turbulence is propagated over a distance of 20 length scales until it reaches the escarpment of the terrain. That is sufficient time to map the anisotropic turbulence cascade in the field [16, 17]. Müller [18] analysed that it takes only a few length scales until the analytical spectrum has adapted to the real flow field with FLOWer. On top of that, the mesh resolution does not change in streamwise direction to prevent grid induced turbulence generation and dissipation.

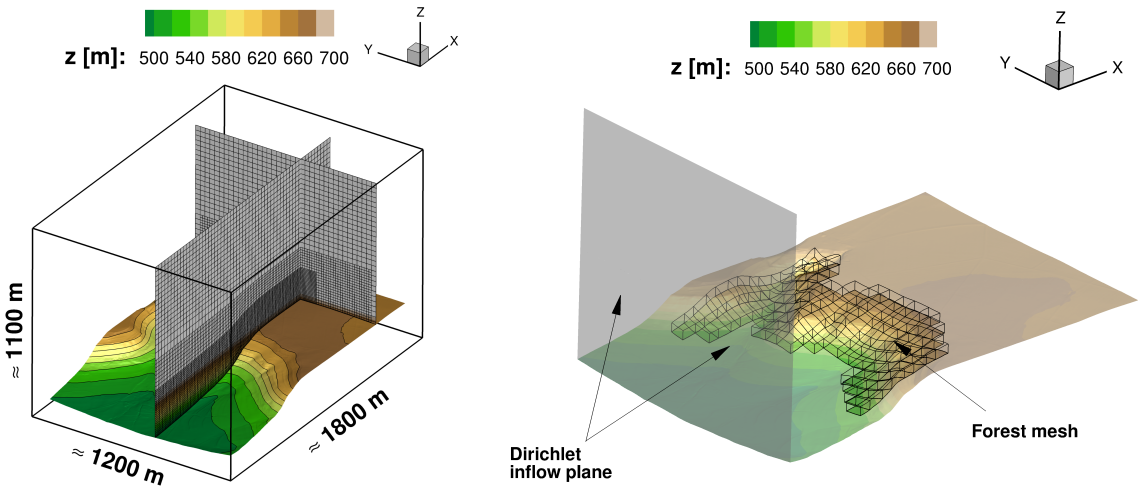

(a) Meshed topography of the test site **(b)** Dirichlet inflow plane and an additional forest mesh

Figure 1: Simulation domain with meshes and setup

2.2. Numerical Methodology

For the current investigation, the compressible flow solver FLOWer [19] is used. This was originally developed at the German Aerospace Center (DLR) and is continuously improved at the IAG in Stuttgart for various applications. Main aspects of these improvements refer to extensions of the code for simulations of atmospheric turbulence in complex terrain sites [12, 17, 20]. The performed FLOWer simulations are Delayed Detached Eddy Simulations (DDES) of the complex terrain site, which form a good compromise between RANS and LES to analyse flow separations and high turbulence intensities due to the topography [21]. The use of a fifth order Weighted Essentially Non-Oscillatory (WENO) scheme enables FLOWer to realize higher accuracies of the turbulent propagation with simultaneously lower dissipation [22]. Previous analyses with the original code using the Jameson-Schmidt-Turkel (JST) scheme [23] showed much more numerical dissipation and problems to satisfactorily resolve turbulent scales. The Menter-SST turbulence model [24] and the Smagorinsky subgrid scale model are applied.
As illustrated in Figure 1 (b), the geometry of the forest is placed into the domain by an additional mesh applying the Chimera technique for overlapping grids [25]. The forest is modeled in FLOWer in analogy to Letzgus [12] and is based on the investigations of Shaw and Schumann [26]. The forest model of OpenFOAM is based on these investigations, too. The laterally averaged Leaf Area Index (LAI) at December was approximately 2, which is typical for mixed forests in winter. The forest height and the local foliage densites vary in height and width and could be chosen in fairly detail in the FLOWer simulations by a digital surface model of the test site that was provided from the State Office for Geoinformation and Land Development Agency (LGL) in Stuttgart. In this way a force term is applied to each cell of the forest mesh based on the surface data of the LGL in order to model the heterogeneous forest and its tree heights and local foliage densities realistically.
As depicted in Figure 1 (a) the mesh could be refined to resolve small eddies of the local flow field in the area of interest by applying hanging grid nodes. This is important especially in the wake of the slope and the forest near the met masts. The finest resolution of the grid is 1m and the coarsest resolution is 4m near the lateral and the upper far field boundary conditions to save computational costs. The outflow boundary condition has been selected as far field, too. This was valid because no pressure stratification occurred above the height due to neglect of buoyancy forces. The bottom topography is treated as a no-slip condition. The applied FLOWer time step for the flow propagation was small in order to ensure a Courant-Friedrich-Lewy (CFL) number smaller than 1. The boundary layer of the FLOWer domain is fully resolved with $y^+ \approx 1$ because no wall model or roughness elements except the forest area were applied. Overall the FLOWer domain contains approximately 250M cells. Each conducted simulation used approximately 7200 CPUs, totaling around 200 hours of computing time. The FLOWer spin-up time was 30 hours until the flow has been propagated through the flow field once.

3. Results

The results show highly resolved FLOWer simulations of the wind energy test site with inflow data from the described model chain. The results are divided in three parts. Firstly, the described inflow conditions are presented and are propagated through the domain. Afterwards, some general results of the turbulent local flow field are discussed. Finally, a quantitative comparison with the two met masts is shown. For the verification of these comparisons, another simulation has been conducted, in which a laterally constant velocity profile was superimposed with the same turbulent fluctuations.

3.1. Inflow

The inflow data plane illustrated in Figure 1 (b) is shown in Figure 2.

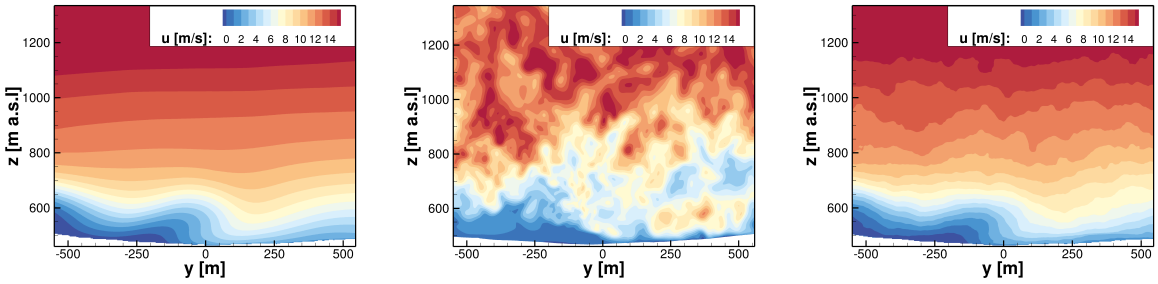

(a) Velocity distribution of the inflow plane provided by precursor OpenFOAM simulations

(b) Velocity distribution of the inflow plane superimposed with synthetic turbulence

(c) Time averaged velocity distribution of the inflow plane over two minutes

Figure 2: Velocity distribution of the FLOWer inflow plane

This Figure outlines the inflow data of the FLOWer simulation. As introduced in section 2, an averaged inflow plane of the streamwise velocity is provided by OpenFOAM. The velocity distribution of this averaged inflow data plane is outlined in Figure 2 (a). The streamwise velocity field with a flow direction perpendicular to this plane is shown. In another step, this inflow plane as well as the mean vertical and lateral velocities are superimposed with unsteady fluctuations based on met mast measurements to receive highly turbulent transient inflow conditions. An instantaneous situation of the unsteady inflow plane is visualised in Figure 2 (b). Near the wall from y=−550m up to y=−220m a low-speed area is visible. These small axial velocities occur due to the wake of a hill modeled in the OpenFOAM domain, which is located upstream of the FLOWer inflow plane. Therefore, this information of the local flow situation upstream of the FLOWer domain is important to simulate the correct inflow conditions in the valley. Compared to previous projects that have simulated a simple superposition of a mean velocity profile with transient fluctuations, the lateral variation of the incoming wind field could be taken into account by this approach. Figure 2 (c) shows a time averaged inflow plane over two minutes. It verifies that in the mean the flow field is similar to the time averaged flow field provided by OpenFoam in Figure 2 (a) despite the highly turbulent flow shown in Figure 2 (b).

3.2. General simulation results

This section presents results of the flow field to give an impression of the flow situation at the test site during the observed time period from 2:40 pm to 2:50 pm, on 09.12.2019. As part of the evaluation of the simulation results, it has been verified that only cells in areas $z < 1$m a.g.l are modeled in URANS mode. The rest of the flow field is completely simulated in LES mode to resolve the turbulent structures and to be able to predict the inflow conditions for the wind turbines as precisely as possible.

A general overview of the test site and the flow conditions is provided in Figure 3. Within this three-dimensional Figure the surface structure of the orography and a vertical plane of the local flow field are visible. The surface is coloured by height above sea levels and the vertical plane is coloured by levels of the horizontal velocity of the wind. Highlighting λ_2 structures written in an area on the flat plateau in the wake of the forest, demonstrates the highly turbulent

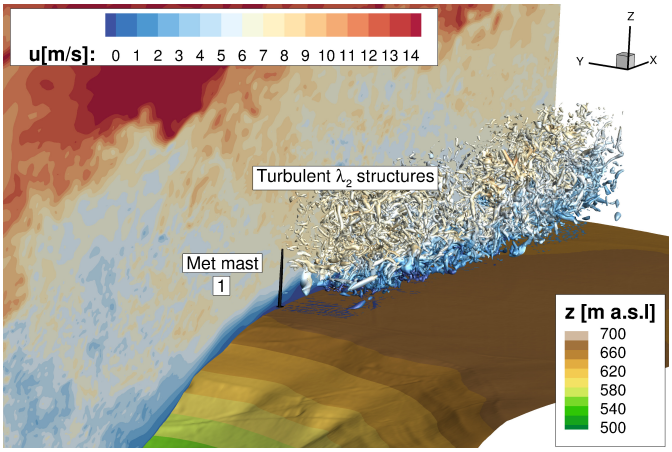

Figure 3: Snapshot of the local flow field situation at the test site. A vertical plane of the instantaneous flow field crosses the position of the met mast

flow situation. To emphasize the turbulent flow situation in the area of interest, the turbulent structures in other regions were hidden in this Figure. Besides, met mast 1 is visualised on the test site to illustrate the general effects that occur at its position. The mentioned effects are high inclination angles, acceleration of the horizontal wind due to the orography, high turbulence intensities and a low-speed area with large turbulent fluctuations near the ground due to the forest wake.

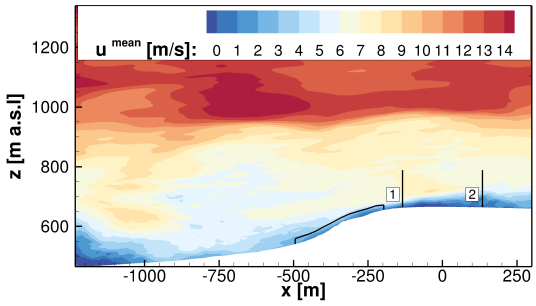

(a) Time averaged flow situation. Met masts and forested area are highlighted

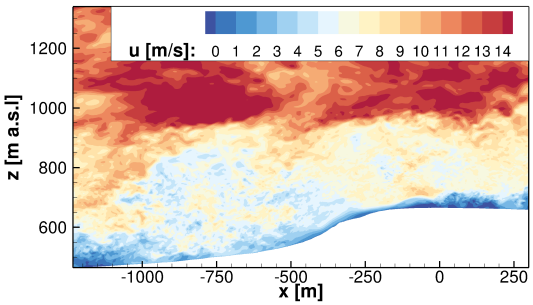

(b) Instantaneous flow situation T1

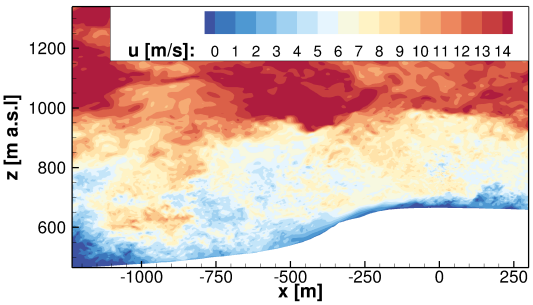

(c) Instantaneous flow situation T2

Figure 4: Flow field situations of the terrain site

Figures 4 (a)-(c) show the flow field in a vertical plane that crosses the designated wind turbine position at x=0m and the met masts at x=−134m (1) and x=134m (2) and simultaneously provides evidence of turbulence characteristics at the met mast positions and further downstream. As shown in Figure 1 (b) the steep slope is fully covered by a dense forest, which results in low wind speeds within the forest at the slope and to a flow separation area near the ground on top of the hill at the flat plateau. The low wind speed area in the valley near the inlet at x ≈ -1300m is due to the wake of a hill modeled in the OpenFOAM domain. The acceleration of the wind speed downstream of the escarpment in the lower flow field up to 800m a.s.l due to the steep slope is clearly visible. Figure 4 (a) shows a time averaged local flow field over one minute and illustrates the positions of the two met masts 1 & 2 and the forested area at the escarpment. Comparisons with measurement data of these two met masts are outlined in the following. Figure 4 (b) and 4 (c) highlight two different arbitrarily chosen instantaneous flow situations. In all of the shown vertical planes an acceleration due to the escarpment is shown. On top of that, the forest and its wake on the flat plateau influence the lower flow field to a large extent. A low-speed area showing high turbulence intensities propagates through the domain. Just behind the forest edge a recirculation area is observed that is also depicted at a time averaged flow situation in Figure 4 (a). The instantaneous flow situations T1 and T2 in Figures 4 (b) and (c) show turbulent vortices detaching from the forest wake, which lead to major differences in instantaneous flow situations on the plateau. Belcher [27] analysed that the flow in the wake of the forest recovers to an atmospheric velocity profile. However, the high turbulence intensities and the mixing of the flows prevent this effect from occuring in the shown simulation domain. For wind turbine wakes, Troldborg [28] argued that the standard deviation decreases further downstream but turbulent structures remain dominant. A similar effect is depicted in Figure 4 for forest wakes. Furthermore, the low-speed area near the ground at the inflow plane described in Figure 2 behaves differently at instantaneous flow situation T1 and T2. It is clearly visible that the height of this low-speed area extends over larger heights in different moments even if, on average, the inflow situation of Figure 2 (a) returns, which was verified by a time averaged inflow plane in Figure 2 (c) . The hill upstream of the FLOWer domain influences the flow propagation to a large amount and leads to low velocities at the valley near the ground, whereas a high-speed streak occurs at approximately z=1000m a.s.l.

3.3. Comparisons with measurement data

Results of the present DDES simulations are compared to measurement data of met masts 1 and 2 at their respective positions.

To evaluate the benefit of superimposing a mean velocity field of previous coarser simulations with turbulent fluctuations, a second simulation has been conducted by superimposing the same turbulent fluctuations with a mean velocity profile that shows spatially constant values in y-direction. This mean velocity profile is extracted from the time averaged OpenFOAM inflow plane in Figure 2 (a) by averaging this plane laterally. Thus, a Hellmann exponent of α=0.28, a mean velocity of u=6.5$^m/_s$ and a reference height of z=100m a.g.l have been applied.

The shown velocity profiles and the curves of the turbulence intensity and the curves of the inclination angle are time averaged and compared to the mean met mast data of the observed 10-minute period. The power spectral density (PSD) of the simulation results and the measurements are compared at a height of z=73m a.g.l, which is the hub height of the two wind turbines.

Figure 5 compares the results of the DDES FLOWer simulation with measurement data of met mast 1. A time averaged comparison of the atmospheric velocity profiles is given in Figure 5 (a). The time averaged velocity profile of the FLOWer simulation is compared at certain positions, where the met mast is equipped with either ultrasonic anemometry or with cup anemometers. The velocity profile of the simulation generally matches with the measured

data at all heights. The small wind speeds near the ground and the inflection point of the mean profile at approximately z=16m a.g.l can be explained by the low wind speeds of the forest wake. The maximum deviation of the simulation and the measurements is approximately 8%. The velocity above z=40 m a.g.l behaves almost constantly for the FLOWer results and the measurement data. The simulation with a laterally constant velocity profile (DDES $\alpha = 0.28$) shows higher speeds at lower altitudes. This can be explained by the fact that the wake of the hill upstream of the FLOWer domain is neglected. The larger deviation from the ultrasonic anemometer at a height of 20m can also be attributed to this effect. At higher altitudes the influence of the hill upstream of the FLOWer domain disappears and the flow of both simulations behave similarly. Figure 5 (b) compares the turbulent statistics of the flow. As described

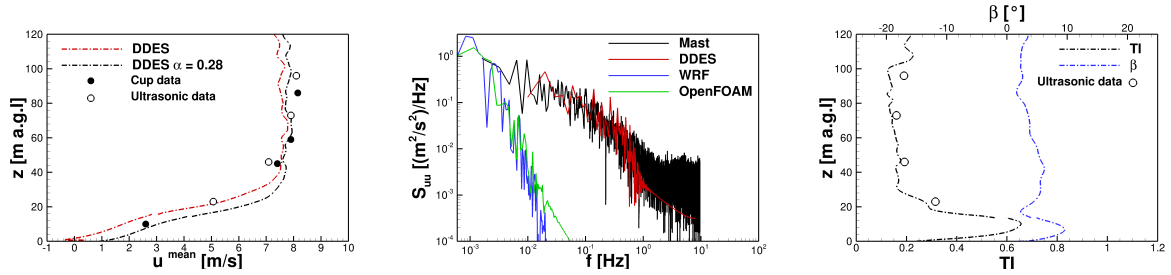

(a) Time averaged atmospheric velocity profiles

(b) Power spectral density (PSD) at z=73m a.g.l

(c) Turbulence intensity TI and inclination angle β

Figure 5: Comparison of DDES and measurements of met mast [1]

in section 2, the turbulence intensities of the met mast can be considered in the simulations by superimposing synthetic turbulence at the inflow. Figure 5 (b) shows the decaying of the turbulence by visualising the power spectral densities S_{uu} of the turbulence at z=73m a.g.l. This height represents the hub height of the two wind turbines that will be installed at the test site. The power spectral densities show a good agreement, especially in the low frequency area below 1Hz. For higher frequencies the simulated small turbulent scales dissipate faster than the measured turbulence of the met mast. To illustrate the need of superimposing turbulent fluctuations to resolve the microscale turbulence, the PSD of the WRF and the OpenFOAM simulations at the hub height is added in this Figure, too. It is obvious that the power spectral densities of WRF and OpenFOAM decay faster than the FLOWer simulations and the measurements, and are therefore not able to resolve the small turbulent scales. In Figure 5 (c) the turbulence intensity of the DDES simulation is compared to measurement data of the ultrasonic anemometers and the curve aligns with the measured data. At 20m, the deviation is greater because the area up to this height shows very high turbulence intensities due to the highly turbulent low-speed forest wake near the ground. On top of that, Figure 5 (c) depicts the inclination angle β of the flow. It is noticeable that the flow is still slightly upward at this position due to the slope inclination. Figure 6 shows the same comparisons for met mast [2]. Figure 6 (a) again outlines an adequate agreement of the time averaged velocity profile with the measured data even if it depicts larger deviations than the comparison in Figure 5 (a). The wind speed reduction of the forest wake seems to be overestimated at this position due to the low wind speeds at z=10m a.g.l compared to the met mast data. The differences of the two DDES simulations decrease further downstream on the flat plateau, so that the two curves are very similar at the height of met mast [2]. The difference between the two inflow planes reduces further downstream on the flat plateau between met mast [1] and met mast [2]. The curves of the power spectral densities in Figure 6 (b) represent again a similar distribution as the spectra of Figure 5 (b) up to a frequency of 1Hz. Figure 6 (b) also shows the power spectral densities

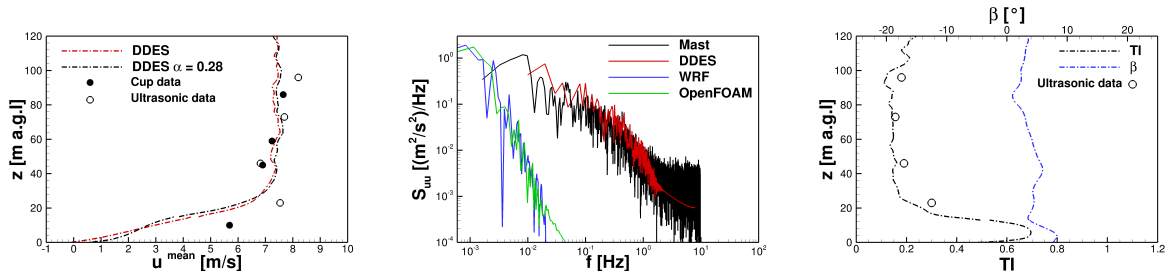

(a) Time averaged atmospheric velocity profiles

(b) Power spectral density (PSD) at z=73m a.g.l

(c) Turbulence intensity TI and inclination angle β

Figure 6: Comparison of DDES and measurements of met mast 2

of WRF and of OpenFOAM at the hub height. It can be seen that the microscale turbulence cannot be captured well, which emphasizes the need to superimpose the synthetic turbulence in FLOWer in order to achieve the TKE at the met mast. Figure 6 (c) again shows the comparison of the tubulence intensity with the measured data and the behaviour of the inclination angle at this position. Both the progression and the relation to the measured data behave similarly to the comparison in Figure 5 (c). Thus, the simulation and the measurements, once more, demonstrate high turbulence intensities. The highly turbulent forest wake again leads to a strong deflection of the turbulence intensity near the ground in this Figure. The inclination angle β shows still a slightly upward flow situation.
Analysing the results of Figure 5 and Figure 6, it can be concluded that the met masts feature high turbulence intensities, which can be represented in the FLOWer simulations. The time averaged velocities have shown that the vertical gradients of the atmospheric velocity profile are low at the hub height of the wind turbines (73m a.g.l) resulting in minor differences of the mean velocity. Thus, lower load differences above the rotor plane are expected in the observed time period. Although, it has to be mentioned that in analogy to Figure 4 the wake of the forest temporarily crosses the lower half of the rotor plane when considering the wind turbines. Hence, load differences of the rotor plane will mainly be based on turbulent fluctuations of the flow and the forest wake. Taking into account Figure 4, it becomes obvious that the forest wake could cross the wind turbine wake leading to a mixing and possibly faster decaying of the turbine wake.

4. Conclusions

This paper discusses Delayed Detached Eddy Simulations of a wind energy test site in the Swabian Alps with the compressible flow solver FLOWer. As part of the project WINSENT, numerical investigations were analysed and compared to the measurement data of the met masts. The inflow data for the highly resolved numerical simulations is provided by a three-part model chain consisting of WRF, OpenFOAM and FLOWer. The FLOWer inflow data provided by OpenFOAM was averaged and afterwards superimposed with fluctuations based on measurements of the met masts to obtain highly turbulent wind field data for the inflow plane of the microscale FLOWer simulations. This unsteady turbulent flow was propagated through the spatially and temporally highly resolved FLOWer domain to simulate real inflow conditions for the designated wind turbines of the test site. In order to achieve this objective, the flow field was initially analysed. Subsequently, the numerical results were compared to measurements of the two already installed met masts of the test site. The shown results exhibit a good agreement of the Delayed Detached Eddy Simulations with the measurements of the two met masts. The time

averaged velocity profiles as well as the power spectral densities of the CFD simulation show a good correspondence to the measurement data. With a second more generic CFD simulation, the numerical model was verified for the present flow field. Comparisons of both simulations with met mast data depicted that the inflow data of this model chain is especially beneficial in the lowest part of the atmospheric boundary layer near the ground. In a next step the wind turbine can be considered for numerical CFD investigations.

Acknowledgments

This research is funded by the *German Federal Ministry for Economic Affairs and Energy* (BMWi) within the framework of the German joint research project "WINSENT" (Code number: 0324129). The authors gratefully acknowledge the support by the research network WindForS and acknowledge the provision of the computational resources of the High Performance Computing Center Stuttgart (HLRS) and the Leibniz Computing Center Munich (LRZ).

References

[1] Windfors URL `https://www.windfors.de/de/startseite/`
[2] Lutz T, Schulz C, Letzgus P and Rettenmeier A 2017 Impact of Complex Orography on Wake Development: Simulation Results for the Planned WindForS Test Site *Journal of Physics: Conference Series* **854** 012029
[3] Wegley H L, Ramsdell J V, Orgill M M and Drake R L 1980 Siting Handbook for Small Wind Energy Conversion Systems *Battelle Pacific Northwest Labs., Richland, WA (USA)*
[4] Emeis S 2012 Wind Energy Meteorology: Atmospheric Physics for Wind Power Generation *Springer Science & Business Media*
[5] Bowen A J and Lindley D 1977 A Wind-Tunnel Investigation of the Wind Speed and Turbulence Characteristics close to the Ground over Various Escarpment Shapes *Boundary-Layer Meteorology* **12** 259–271
[6] Schulz C, Hofsäß M, Anger J, Rautenberg A, Lutz T, Cheng P W and Bange J 2016 Comparison of Different Measurement Techniques and a CFD Simulation in Complex Terrain *Journal of Physics: Conference Series* **753** 082017
[7] Berg J, Mann J, Bechmann A, Courtney M and Jørgensen H E 2011 The Bolund Experiment, Part I: Flow over a Steep, Three-Dimensional Hill *Boundary-layer meteorology* **141** 219
[8] Finnigan J J and Belcher S E 2004 Flow over a Hill covered with a Plant Canopy *Quarterly Journal of the Royal Meteorological Society* **130** 1–29
[9] Brodeur P and Masson C 2008 Numerical Site Calibration over Complex Terrain *Journal of Solar Energy Engineering* **130** 031020
[10] Bechmann A and Sørensen N N 2010 Hybrid RANS/LES Method for Wind Flow over Complex Terrain *Wind Energy* **13** 36–50
[11] Schulz C, Klein L, Weihing P and Lutz T 2016 Investigations into the Interaction of a Wind Turbine with Atmospheric Turbulence in Complex Terrain *Journal of Physics: Conference Series* **753** 032016
[12] Letzgus P, Lutz T and Krämer E 2018 Detached Eddy Simulations of the local Atmospheric Flow Field within a Forested Wind Energy Test Site located in Complex Terrain *Journal of Physics: Conference Series* **1037** 072043
[13] Storm B, Dudhia J, Basu S, Swift A and Giammanco I 2009 Evaluation of the Weather Research and Forecasting model on forecasting Low-Level Jets: Implications for Wind Energy *Wind Energy* **12** 81–90
[14] Mann J 1994 The spatial structure of neutral atmospheric surface layer turbulence *Journal of Fluid Mechanics* **273** 141–168
[15] Peña A, Gryning S E and Mann J 2010 On the Length-Scale of the Wind profile *Quarterly Journal of the Royal Meteorological Society* **136** 2119–2131
[16] Kim Y, Schwarz E, Bangga G, Weihing P and Lutz T 2016 Effects of Ambient Turbulence on the Near Wake of a Wind Turbine *Journal of Physics: Conference Series* **753**
[17] Schulz C, Meister K, Lutz T and Krämer E 2016 Investigations on the Wake Development of the Mexico Rotor considering different Inflow Conditions *Springer International Publishing* 871–882
[18] Müller J, Lutz T and Krämer E 2020 Numerical Simulation of the Swept FNG Wing in Atmospheric Turbulence *AIAA AVIATION 2020 FORUM*

[19] Kroll N, Rossow C C, Becker K and Thiele F 2000 The MEGAFLOW Project *Aerospace Science and Technology* **4** 223–237
[20] Meister K, Lutz T and Krämer E 2014 Simulation of a 5MW Wind Turbine in an Atmospheric Boundary Layer **555** 012071
[21] Weihing P, Letzgus J, Bangga G, Lutz T and Krämer E 2018 Hybrid RANS/LES Capabilities of the Flow Solver FLOWer - Application to Flow Around Wind Turbines *Progress in Hybrid RANS-LES Modelling* 369–380
[22] Schäferlein U, Keßler M and Krämer E 2013 High Order CFD-Simulation of the Rotor-Fuselage Interaction *39th European Rotorcraft Forum* 37–39
[23] Jameson A Time Dependent Calculations using Multigrid, with Applications to Unsteady Flows past Airfoils and Wings *AIAA paper* **1596** 1991
[24] Menter F 1994 Two-Equation Eddy-Viscosity Turbulence Models for Engineering Applications *AIAA journal* **32** 1598–1605
[25] Benek J A, Steger J L, Dougherty F C and Buning P G 1986 Chimera. A Grid-Embedding Technique Tech. rep. AEDC-TR-85-64, Arnold Engineering Development Center
[26] Shaw R H and Schumann U 1992 Large-eddy Simulation of Turbulent Flow above and within a Forest *Boundary-Layer Meteorology* **61** 47–64
[27] Belcher S, Harman I and Finnigan J 2012 The Wind in the Willows: Flows in Forest Canopies in Complex Terrain *Annual Review of Fluid Mechanics* **44** 479–504
[28] Troldborg N, Sorensen N, Norkaer J and Mikkelsen R F 2008 Actuator Line Modeling of Wind Turbine Wakes *Dissertation*